RASĀYAN *J. Chem.*
Vol. 16 | No. 1 |325-334| January - March | 2023
ISSN: 0974-1496 | e-ISSN: 0976-0083 | CODEN: RJCABP
http://www.rasayanjournal.com
http://www.rasayanjournal.co.in

HYDROGEN PRODUCTION FROM ETHANOL BY STEAM REFORMING OVER NICKEL AND COBALT GEOTHERMAL WASTE SUPPORTED CATALYST

J. Philia[1,3], W. Widayat[1,2,3,✉] and S. Sulardjaka[1,3]
[1]Department of Mechanical Engineering, Diponegoro University, 50275, Indonesia
[2]Center of Biomass and Renewable Energy, Diponegoro University, 50275, Indonesia
[3]Advance Materials Laboratory Center of Research and Service Unit, Diponegoro University, 50275, Indonesia
✉Corresponding Author: widayat@live.undip.ac.id

ABSTRACT
Hydrogen production was studied over nickel and cobalt geothermal waste-supported catalysts. Due to their good catalytic activity, nickel, and cobalt are widely used as catalysts in ethanol steam reforming. The geothermal waste catalyst (GWC) was synthesized by hydrothermal process, then prepared using wet-impregnation with nickel nitrate and cobalt nitrate as the precursors. SEM analysis shows that nickel and cobalt successfully adhered to the GWC, which decreased the surface area. Using nickel and cobalt in ethanol steam reforming produces a higher hydrogen yield than a GWC. The best hydrogen yield was 43.04% over Ni/GWC at 550°C. Nickel can actively break C-C, O-H, and C-H bonds to produce hydrogen and reduces the brønsted acid site as the carbon formation active site.
Keywords: Hydrogen, Geothermal Waste, Steam Reforming, Ethanol, Transition Metal.
RASĀYAN *J. Chem.*, Vol. 16, No.1, 2023

INTRODUCTION

Global warming and the decline in petroleum-based energy are problems in the 4.0 Industry era. The ability to fulfill the energy needs while reducing greenhouse gas emissions is needed to deal with these problems. Hydrogen is the lightest element in the universe the element has greater combustion energy than other fuels. Hydrogen can be applied as an alternative fuel for internal combustion engines, gas turbines, and fuel cells, enabling these applications to work with high efficiency and low pollution.[1] The only by-products of hydrogen combustion are water vapor and energy, making hydrogen a particularly clean and efficient renewable energy source.[2] Hydrogen is a new renewable energy resource, significantly reducing the use of fossil fuels and greenhouse gases. To this date, 95% of hydrogen production is carried out using fossil fuels, namely natural gas. Non-fossil materials such as ethanol can be a potential raw material to produce hydrogen to substitute natural gas utilization. Due to the high efficiency of the ethanol steam reforming process, it does not require a high ethanol concentration.[3] The catalytic activity of the ethanol steam reforming process is also determined by the type of support used in the catalyst. One type of catalyst support that can be used for this process is silica-alumina, which increases the steam-reforming catalytic activity. Silica-alumina catalyst has a large surface area, so the metal (Ni,Cu, Zn) is evenly dispersed, increasing the catalytic activity of methanol production.[4,5] The geothermal power plant process produces waste, where the results of the silica and other mineral levels analyses show its potential as a raw material for silica-aluminum catalysts.[6,7] Indonesia has 13 Geothermal Power Plants spread across various regions based on the data from the Ministry of Energy and Mineral Resources in 2018, which shows that the amount of geothermal waste in Indonesia is large, whereas the processing of geothermal waste has not been maximized.[8] Hydrogen synthesis using ethanol steam reforming with a catalyst derived from geothermal waste has not yet been investigated. Nickel and cobalt metals are widely used as catalysts in the steam reforming process because they have good catalytic activity as previously reported by Cheng & Dupont (2017) on ethanol steam reforming process to produce hydrogen using 18NiO/α-Al_2O_3 catalyst. The hydrogen product yield is 25% with a conversion of 91% at an operating temperature of 650°C.[9] Zhurka *et al.* (2018) obtained 35% hydrogen yield and 100% conversion at 500°C temperature reaction with 10Ni/SiO_2 catalyst.[10] Alumina support catalyst with cobalt (5Co/α-Al_2O_3) is also used for hydrogen production trough ethanol steam

http://doi.org/10.31788/RJC.2023.1616808

reforming at 550°C with 43% of ethanol conversion and 28% of hydrogen yield.[11] Riani *et al.* (2018) obtained a hydrogen yield of 64% and a conversion of 86% at a lower temperature of 500°C using a 17Co/α-Al_2O_3 catalyst.[12] Based on the previous research, nickel and cobalt are often used for ethanol steam reforming catalysts with silica or alumina as support, while the silica-alumina from geothermal waste for nickel and cobalt catalysts has not been utilized. In this research, geothermal waste catalyst (GWC) is synthesized by hydrothermal process and impregnated with nickel and cobalt. Functional group, crystal structure, surface area, pore distribution and surface morphology of the catalysts are characterized. The catalysts activity on the hydrogen production are evaluated at a fixed bed reactor trough ethanol steam reforming. The water content in ethanol used as fuel can damage engine performance, so fuel-grade ethanol (99.5-100% concentration) is widely used as an alternative fuel to replace fossil energy, however the ethanol purification process to achieve fuel-grade requirements requires high equipment and operating costs.[13] Hence, the hydrogen production using ethanol 80% in order to reduce fossil energy dependency by economic raw material.

EXPERIMENTAL

Materials

PT. Geo Dipa Energi Geothermal Power Plant in Dieng, Wonosobo, Indonesia supplied the geothermal solid waste for GWC raw material. Whereas, the catalyst production and impregnation, sodium hydroxide (NaOH, 99%), aluminum hydroxide ($Al(OH)_3$, 99.63%), nickel (II) nitrate hexahydrate ($Ni(NO_3)_2.6H_2O$, for analysis), and cobalt (II) nitrate hexahydrate ($Co(NO_3)_2.6H_2O$, for analysis) were acquired from Sigma Aldrich, Germany. Indrasari Chemical Store was the supplier of the 96% ethanol utilized for steam reforming. The availability of nitrogen gas (N_2, 99.9%) from PT. Samator Gas. The Centre of Research and Services-Diponegoro University supplied Aquadest.

Catalyst Synthesis

The washed and dried geothermal waste was crushed and sieved to 125 microns. In the stirred tank reactor, 400 grams of $Al(OH)_3$ and 1000 grams of sieved geothermal waste were combined with 4 liters of NaOH 3M solution. The hydrothermal period takes eight hours while the solution is stirred at 250 rpm and 100°C to produce a silica-alumina phase with a porous surface.[14] After the hydrothermal process, it was cooled for 12 hours at room temperature. To ensure water elimination, the hydrothermal product was subsequently dried in an oven (MTI, EQ-6020-FP, USA). A tube furnace (Lindberg/Blue M, Asheville, North Carolina, United States) was operated for 6 hours at 550°C to remove impurities and carbon from the catalyst. The geothermal waste-derived catalyst was denoted GWC. Impregnated catalysts were prepared using the wet impregnation method with nickel ($Ni(NO_3)_2.6H_2O$) and cobalt ($Co(NO_3)_2.6H_2O$) as the precursors. In 100 mL of aquadest, the metal salt of 2% by mass GWC was dissolved, then GWC was added and stirred at 60°C 500 rpm for 6 hours. The catalysts were separated by filtering after a 12-hours precipitation period. After the 12h of precipitation, the catalysts were dried in an oven (MTI, EQ-6020-FP, USA) at 105°C overnight. In order to remove organic compounds and impurities, the catalysts were calcined for 6 hours at 550°C in a tube furnace (Lindberg/Blue M, Asheville North Carolina, USA). The catalysts were labeled as Ni/GWC, Co/GWC and NiCo/GWC.

Catalyst Characterization

Fourier-Transform Infrared Spectroscopy (FTIR) analysis was conducted to identify the functional group of the catalysts using Perkin Elmer Spectrum Two IR. To study the structure and crystallinity of the catalyst, X-ray Diffraction (XRD) was used by Shimadzu XRD-7000 with Cu K-ray radiation as the X-ray source with a voltage of 30 kV and a current of 30 mA. X'Pert High Score PANalytical was used in the XRD interpretation. Catalysts morphology, elemental identification and quantitative compositional information were examined by JEOLJSM-6510LA Scanning Electron Microscopy (SEM) with Energy Dispersive X-Ray Analyzer (EDX) at an accelerating voltage of 20 kV. The surface area and pore size distribution of Ni/GWC, Co/GWC, and NiCo/GWC were studied by nitrogen (N_2) adsorption-desorption using Quantachrome Autosorb-iQ. The surface area calculation was carried out using BET method, while the pore size distribution by BJH method.

Ethanol Steam Reforming

The catalysts' activity and selectivity for ethanol steam reforming were tested using a stainless-steel fixed bed reactor (inside diameter 2 cm). Before the experiments, 2 grams of catalyst was loaded into the reactor with both ends was plugged by glass wool. The catalyst activity tests were conducted at temperatures 500°C, 550°C, 600°C and 625°C, where the reactor was heated by a vertical tube furnace equipped with a K-type thermocouple. Ethanol 80% was evaporated until the pressure inside the evaporator reached 12 psi, then driven into the reactor by nitrogen gas. The product gas from the reactor was analyzed by a gas analyzer (Tecnotest Stargas 898, France) to determine the composition, then led through a cooling condenser to obtain a liquid product for GCMS analysis (Shimadzu GCMS-QP2010 SE).

The catalyst selectivity forwards H_2 was defined as eqn.-1.

$$S_{H_2} = \frac{n_{H_2}^{out}}{n_{C_2H_5OH}^{out} - n_{C_2H_5OH}^{in}} \text{ x } 100 \quad (1)$$

Where $n_{C_2H_5OH}^{in}$ is the input molar flow rate of ethanol, $n_{C_2H_5OH}^{out}$ and $n_{H_2}^{out}$ are the molar flowrate of ethanol and hydrogen, respectively.

RESULTS AND DISCUSSION

Catalyst Characterization

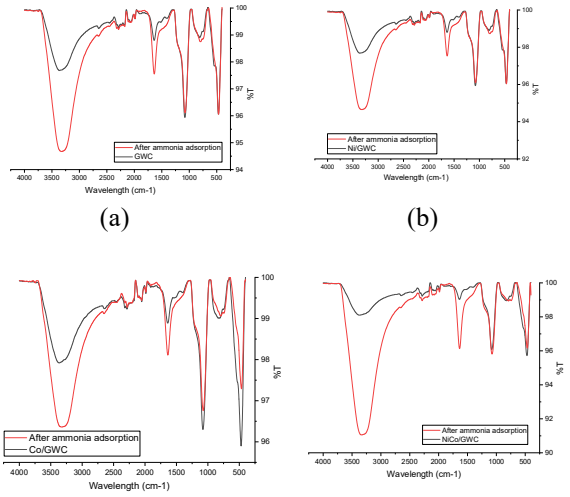

Fig.-1: Infrared Spectra of (a)GWC (b)Ni/GWC (c)Co/GWC (d)NiCo/GWC

The IR spectra of the GWC in the region 4000-250 cm^{-1} are shown in Fig.-1. According to the FTIR experimental data, a peak between 3200 - 3700 cm^{-1} indicated the presence of water caused by the stretching vibration of the hydroxyl (OH) group of silanol (Si-OH). A peak at 1636 cm^{-1} confirms that the bending vibration of the OH group caused the presence of water.[15] The peaks at 798 cm^{-1} and 1081 cm^{-1} are the results of the symmetry and asymmetry stretching of Si-O-Si, which indicates that silica has not completely reacted with alumina and indicates the amorphous silica component. The peak found at 466 cm^{-1} is characterized as pseudo-boehmite stretching vibration. Pseudo-boehmite is a low crystalline aluminum hydroxide with AlO(OH) chemical composition.[16,17,18] These findings indicated that the hydrothermal process at the temperature of 100°C had not reacted perfectly with Si and Al, so a higher temperature is needed to react Si and Al into aluminosilicate crystals completely.[19,20]

Table-1: Hydroxyl Group Area

Catalyst	Area (%T)
GWC	929.17
Ni/GWC	1754.59
Co/GWC	1196.31
NiCo/GWC	3015.57

GWC is a solid material with Brønsted and Lewis acid sites which play an essential role in catalytic activity. The Brønsted acid site is a site that can release H^+ ions or often referred to as protonic acid, while the Lewis acid site is a site that can accept a pair of electrons. The determination of the acidity of the GWC can be done by using the adsorption technique of ammonia as an adsorbate base followed by analysis using FTIR. Table-1 presents the area of the hydroxyl group at a wavelength of 3200-3700 cm^{-1} by the red line. Based on calculations using the PerkinElmer Spectrum IR software, the area of the hydroxyl group NiCo/GWC > Ni/GWC > Co/GWC > GWC. The area of the hydroxyl group at a wavelength of 3200-3700 cm^{-1} shows the characteristics of an acidic site on the GWC.[14,15] A peak at 3200-3700 cm^{-1} indicates the interaction between the catalyst's ammonia adsorbate base and the Lewis acid site. This interaction represents the amount of Lewis acid site on the catalyst.[21] The hydroxyl group area of the catalysts shows that nickel and cobalt increased the Lewis acid site in the catalyst. The IR spectra found in Ni/GWC, Co/GWC and NiCo/GWC did not show significant differences with GWC. Nickel particles in the GWC can be indicated by the presence of Ni-O vibrational peak at the wavelengths of 419 cm^{-1} and 614 cm^{-1}, while Co-O stretching vibration at 567 cm^{-1} indicates the presence of cobalt.[22,23] Based on the spectrum of the impregnated GWC, there was no peak at the wavelength, indicating the presence of nickel and cobalt. The IR spectra of the catalyst is align with the XRD result, where the presence of nickel and cobalt cannot be identified due to the small amount of metal used for impregnation.[24] Peaks identified the Al_2O_3 peaks were detected at 2Theta (2θ) 37.66°, 46.03° on GWC, 37.29°, 42.56° on Co/GWC, and 37.61°, 45.77° onNi/GWC, while peaks at 67.35° on the catalysts belonging to Na-β-alumina ($Na_{1.68}Al_{11}O_{17}$) phase.

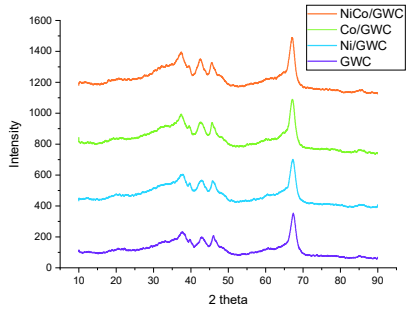

Fig.-2: Diffractogram of The Catalysts

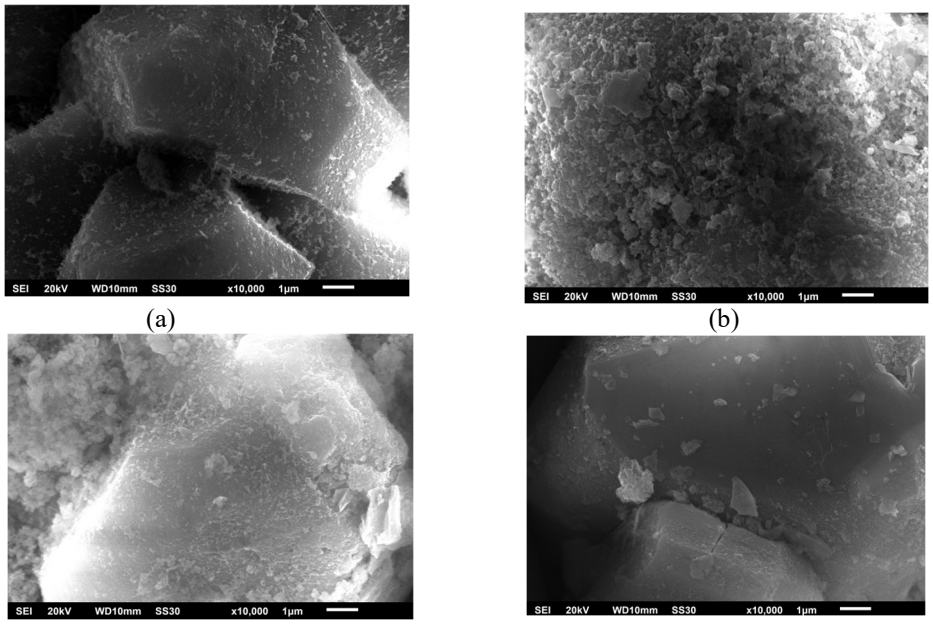

Fig.-3: Morphology of (a) GWC (c) Ni/GWC (c) Co/GWC (d) NiCo/GWC by SEM Analysis with 10000x Magnification

Figure-3(a) shows the morphological characterization of the GWC catalyst using SEM, in which the morphological structure of the GWC resembles a pentagon with irregular sides. Figure-3(b, c, and d) shows the differences in surface morphology of the catalysts because of the impregnation. GWC is a porous material that allows the metal to be evenly dispersed on the surface.[20] The lumps that cause the uneven surface in the two images are nickel and cobalt adhering to the GWC surface.

Table-2: SEM-EDX Analysis of Catalyst

Catalyst	Component (%mass)			
	Al_2O_3	SiO_2	NiO	CoO
GWC	82.40	4.17	-	-
Ni/GWC	58.75	21.57	1.83	-
Co/GWC	68.59	7.43	-	1.03
NiCo/GWC	74.24	5.81	1.13	0.52

The results of the SEM-EDX analysis show that nickel and cobalt were impregnated, but only a small amount of metal was attached to the catalyst. These cause no nickel and cobalt peaks found in the IR spectra and diffractogram of the catalyst. The small amount of metal impregnated is due to the low interaction between metal and support catalyst. The low amount of nickel and cobalt can be influenced by the formation of complex compounds involving the two metals, whereas in the EDX analysis, only nickel oxide (NiO) and cobalt oxide (CoO) were detected.[25,26,27] Strong interaction between nickel and support catalyst is formed due to the merging of nickel ions into the tetrahedral vacancies. The limitation of tetrahedral vacancies in β-Al_2O_3 caused nickel weakly interacts with this support.[28] The synthesized catalyst also contains silica (SiO_2) from the geothermal waste of 4.17% in GWC, 21.57% in Ni/GWC, 7.43% in Co/GWC and 5.81% in NiCo/GWC. Whereas, the alumina composition in the GWC is 82.40%, Ni/GWC 58.75%, Co/GWC 68.59% and NiCo/GWC 74.24%. The silica content contained in the catalyst is still low, this is caused by the operating temperature, which is not high enough. The higher the operating temperature, the reaction between silica, NaOH and $Al(OH)_3$ becomes more optimal to produce a product with the main component of silica and alumina. Alumina is often used as a supported catalyst for ethanol steam reforming because it has mechanical, physical and chemical stability that produces hydrogen effectively. Silica is also adequate for hydrogen production due to its large surface area and high-temperature stability. Silica-alumina as a support catalyst would increase the catalytic activity because of its stability, larger surface acid groups, and reduced coke deposition.[29] The operating time affects the amount of silica that can be extracted from geothermal waste, the longer the operation time, the higher the silica composition produced and will reach a constant point under certain conditions. Sumari *et al.* (2020) research showed that the synthesis process of extracting silica from beach sand increased silica composition with increasing time from 3 to 48 hours. Liquid sodium silica ($Na_2O.SiO_2$) is produced from the reaction of geothermal silica and NaOH solution, which was not completely reacting with $Al(OH)_3$ because of limited hydrothermal time.[30,31]

Table-3: Spesific Surface Area by BET Method

Catalyst	Spesific Surface Area (m^2/g)
GWC	276.48
Ni/GWC	158.95
Co/GWC	154.64
NiCo/GWC	107.95

Table-3 shows that nickel and cobalt impregnation decreased the specific surface area of the catalyst. The specific surface area of GWC is 276.48 m^2/g, while Ni/GWC 158.95 m^2/g, Co/GWC 154.64, and NiCo/GWC 107.95 m^2/g. Decreasing of the specific surface area of the impregnated catalyst caused by the adhering of nickel and cobalt on the catalyst surface.[32] This result follows the SEM analysis, in which nickel and cobalt were scattered on the surface of the catalyst.

Ethanol Steam Reforming Using Geothermal Waste Catalyst

The catalytic activity test for the ethanol steam reforming process was conducted in a fixed-bed reactor. Ethanol steam reforming produces gas products that are tested directly using a gas analyzer and stored for

further testing using GCMS. The hydrogen gas product tested using GCMS showed the presence of hydrogen with a chromatogram peak at a retention time of 1.797 minutes, as shown in the Fig.-4. Meanwhile, gas product testing with a gas analyzer shows the gas composition, CO, CO_2, and hydrocarbon.

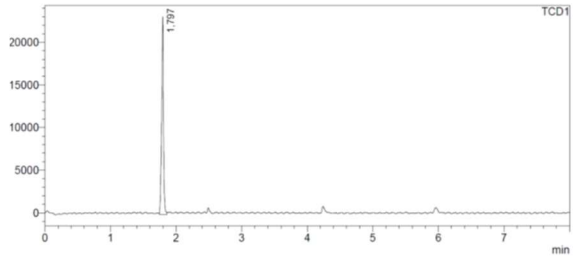

Fig.-4: GCMS Analysis of Gas Product

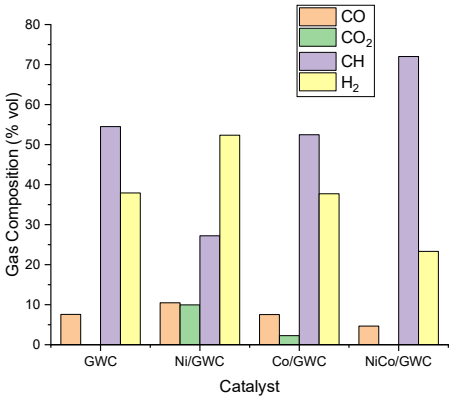

(a)

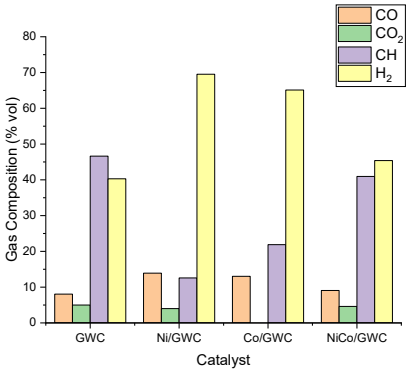

(b)

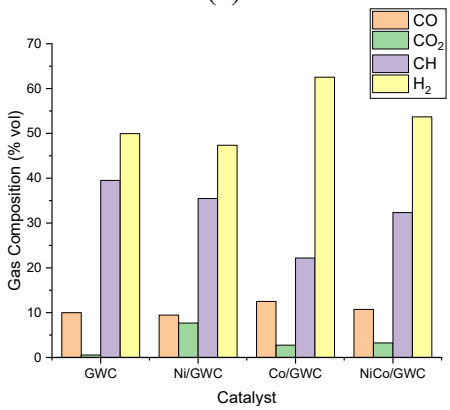

(c)

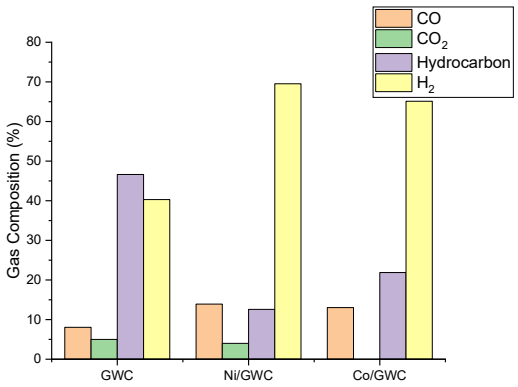

(d)

Fig.-5: Gas Composition of Ethanol Steam Reforming Product at (a)500ºC (b)550ºC (c)600ºC (d)625ºC

Figure-5 shows the yield of ethanol steam reforming gas products uses GWC, Ni/GWC, Co/GWC, and NiCo/GWC. At various temperatures, steam reforming using Ni/GWC produces a hydrogen yield greater than another gas. This proves that nickel can regulate the production of hydrogen during ethanol steam reforming. Nickel as an ethanol steam reforming catalyst can actively break C-C, O-H, and C-H bonds to produce hydrogen and reduces the brønsted acid site as the carbon formation active site.[20,33,34] Ni/GWC produces the highest hydrogen yield of 43.4% at a temperature of 550ºC. Whereas, the highest hydrogen production in ethanol steam reforming using a Co/GWC was obtained at the temperature of 550ºC, which was 38.38%. Cobalt has a $3d^7$ electron configuration, which means that the d subshell valence electrons are not filled. The d orbitals electrons presence, along with the s and p orbitals electronic states, influence the cobalt catalytic activity, leading to a wide variety of low-energy electronic states. In addition, unoccupied orbitals can serve as metal catalytic sites for the production of hydrogen.[33,35] NiCo/GWC produced in a lower hydrogen composition than Ni/GWC at temperatures of 500ºC and 550ºC. However, using a NiCo/GWC resulted in lower CO_2 by-products. The low formation of CO_2 is caused by using a combination of nickel and cobalt metals to increase catalytic activity and catalyst stability, so there is no carbon formation.[26]

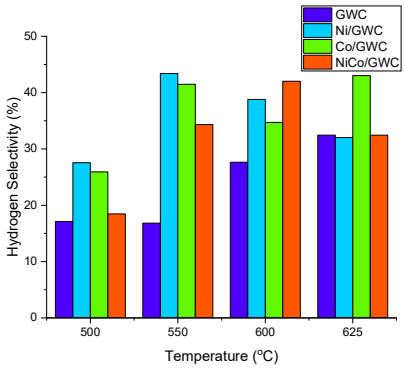

Fig.-6: Hydrogen Selectivity of Ethanol Steam Reforming

Figure-6 shows the hydrogen selectivity of the ethanol steam reforming process using GWC, Ni/GWC, Co/GWC and NiCo/GWC as catalysts. The hydrogen selectivity using nickel and cobalt catalysts at various temperatures is higher than GWC. Ethanol steam reforming was carried out by Lu *et al.* (2019) using a nickel catalyst with a MgO, ZnO, ZrO, and Al_2O_3 buffer catalyst to produce 29%-35% hydrogen.[36] This value is greater than the amount of hydrocarbon produced. GCMS analysis of the liquid product resulting from ethanol steam reforming using GWC showed a diethyl ether compound with a chromatogram peak at the retention time of 1.338 minutes, as shown in Fig.-4. The presence of diethyl ether in the product of ethanol steam reforming using GWC indicates that nickel and cobalt metals produced higher hydrogen selectivity.[4,37] Riani *et al.* (2019) used α-Al_2O_3 and Co/ α-Al_2O_3 catalysts for ethanol steam reforming at

various operating temperature.[12] The reaction using α-Al_2O_3 at a temperature of 250°C-500°C does not produce hydrogen, but the resulting compound is diethyl ether. Whereas, the reaction using a Co/α-Al2O3 catalyst produced up to 56% hydrogen products. During the ethanol steam reforming process, the decomposition of acetaldehyde as a product of ethanol dehydrogenation produces methane with the following reactions :

Ethanol Dehydrogenation

$$C_2H_5OH_{(g)} \rightarrow CH_3CHO_{(g)} + H_{2(g)}$$

Acetaldehyde Decomposition

$$CH_3CHO_{(g)} \rightarrow CH_{4(g)} + CO_{(g)}$$

Ethanol dehydration to diethyl ether occured as a side reaction of the ethanol steam reforming process with the following reaction :

$$2C_2H_5OH_{(g)} \rightarrow C_2H_5OC_2H_{5(g)} + H_2O_{(g)}$$

The Effect of Steam Reforming Temperature on Hydrogen Production

Ethanol steam reforming into hydrogen using GW shows that the higher the reactor temperature, the higher the product. The highest hydrogen yield was obtained at 32.46% v/v at a reactor temperature of 625°C using a GWC. Ethanol steam reforming using a GWC at a temperature of 500°C produces hydrocarbon products, so the hydrogen produced is still low as shown in the Fig.-7. The resulting hydrocarbons may come from acetaldehyde's decomposition reaction and ethanol's dehydration. Widayat *et al.* (2012) performed ethanol steam reforming using a natural zeolite catalyst at a temperature of 140°C, producing a diethyl ether product.[38]

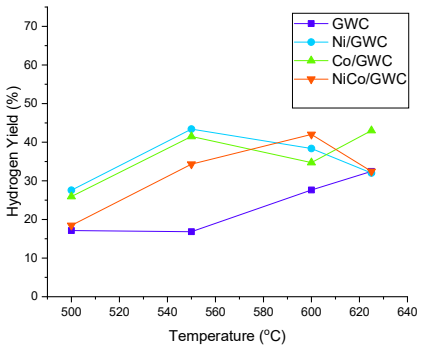

Fig.-7: Hydrogen Yield of Ethanol Steam Reforming

Ethylene (C_2H_4) and diethyl ether ($(C_2H_5)_2O$) are produced through the ethanol steam reforming process using a Co/γ-Al_2O_3 catalyst at a temperature of 200°C – 500°C.[39] The decomposition reaction of acetaldehyde produces methane (CH_4) and carbon monoxide (CO). CH_4 selectivity increases from 400°C to 500°C, then decrease followed by an increase in CO selectivity at temperatures above 500°C.[5,40] Temperature increase induces an increase in hydrogen product through the shift conversion reaction as follows:

$$CO + H_2O \rightarrow CO_2 + H_2$$

Hydrogen yield produced by ethanol steam reforming using Ni/GWC, NiCo/GWC and NiCo/GWC at temperatures of 500°C, 550°C, 600°C and 625°C have higher than using a GWC. Nickel and cobalt as the active site of the GWC can increase the hydrogen selectivity, so that a larger hydrogen product is produced at a lower reactor temperature.[41]

CONCLUSION

Synthesis of a geothermal waste catalyst supported by nickel and cobalt by a hydrothermal process at an operating temperature of 100°C for 8 hours produces alumina and Na-β-alumina crystal phases. The nickel and cobalt were impregnated successfully to the geothermal waste catalyst as shown by SEM-EDX and BET analysis. Ethanol steam reformation with GWC, Ni/GWC, Co/GWC and NiCo/GWC produced the highest hydrogen products of 32.46%, 43.39%, 43.03%, and 42.03%. Ethanol steam reforming over Ni/GWC at 550°C produced the highest hydrogen yield because it enhanced hydrogen selectivity.

ACKNOWLEDGMENTS

The Ministry of Research Technology and Higher Education of the Republic of Indonesia funds this research through the Master's Education toward Doctorate for Excellent Bachelor Program (Grant no. SPK 642-10/UN7.6.1/PP/2021).

CONFLICT OF INTERESTS

The authors declare that there is no conflict of interest.

AUTHOR CONTRIBUTIONS

All the authors contributed significantly to this manuscript, participated in reviewing/editing and approved the final draft for publication. The research profile of the authors can be verified from their ORCID ids, given below:

J. Philia https://orcid.org/0000-0003-3032-1705
W. Widayat https://orcid.org/0000-0003-1906-2378
S. Sulardjaka https://orcid.org/0000-0001-8273-0469

REFERENCES

1. X. Xu, Q. Zhou, and D. Yu, *International Journal of Hydrogen Energy*, **47(79)**, 33677(2022), https://doi.org/10.1016/j.ijhydene.2022.07.261
2. M. Ridwan, D. Suhanda, I. Aziz, and I. Abdullah, *Rasayan Journal of Chemistry*, **14(3)**, 1821(2021), https://doi.org/10.31788/RJC.2021.1436319
3. J. L. Contreras, J. Salmones, J. A. Colín-Luna, L. Nuño, B. Quintana, I. Córdova, B. Zeifert, C. Tapia and G.A.Fuentes, *International Journal of Hydrogen Energy*, **39(33)**, 18835(2014), https://doi.org/10.1016/j.ijhydene.2014.08.072
4. S. Ogo and Y. Sekine, *Fuel Processing Technology*, **199**, 106238(2020), https://doi.org/10.1016/j.fuproc.2019.106238
5. B. Cifuentes, M. F. Valero, J. A. Conesa, and M. Cobo, *Catalysts*, **5(4)**, 1872(2015), https://doi.org/10.3390/catal5041872
6. S. Silviana, G. J. Sanyoto, A. Darmawan, and H. Sutanto, *Rasayan Journal of Chemistry*, **13(3)**, 1692(2020), https://doi.org/10.31788/RJC.2020.1335701
7. J. Philia, W. Widayat, and S. Sulardjaka, *Journal of Environmental Engineering and Science*, **18(1)**, 1(2022), https://doi.org/10.1680/jenes.21.00082
8. N. A. Pambudi, *Renewable and Sustainable Energy Reviews*, **81**, 2893(2018), https://doi.org/10.1016/j.rser.2017.06.096
9. F. Cheng and V. Dupont, *Catalysts*, **7(4)**, (2017), https://doi.org/10.3390/catal7040114
10. M. D. Zhurka, A. A. Lemonidou, J. A. Anderson, and P. N. Kechagiopoulos, *Reaction Chemistry and Engineering,* **3(6)**, 883(2018), https://doi.org/10.1039/c8re00145f
11. S. Ogo, S. Maeda, and Y. Sekine, *Chemistry Letters*, **46(5)**, 729(2017), https://doi.org/10.1246/cl.170072
12. P. Riani, G. Garbarino, F. Canepa, and G. Busca, *Journal Chemical Technology and Biotechnology*, **94(2)**, 538(2019), https://doi.org/10.1002/jctb.5800
13. Y. Sudiyani, S. Aiman and D. Mansur, Perkembangan Bioetanol G2: Teknologi dan Perspektif, LIPI Press, Jakarta(2019)
14. G. Busca, Heterogeneous Catalytic Materials, 1 (2014)
15. L. F. Isernia, *Material Research*, **16(4)**, 792(2013), https://doi.org/10.1590/S1516-14392013005000044
16. D. Liu, P. Yuan, H. Liu, J. Cai, D. Tan, H. He, J. Zhu, T. Chen, *Applied Clay Science*, **80–81**, 407(2013), https://doi.org/10.1016/j.clay.2013.07.006

17. I. M. Yaya, N. Guillaume, and M. Arkhis, *Material Science : An Indian Journal*, **16(3)**, 1(2018)
18. X. Ren, Y. Liu, and L. Miao. *Nanomaterials*, **10(2)**, 263(2020), https://doi.org/10.3390/nano10020263
19. T. A. B. Prasetyo and B. Soegijono, *Journal of Physics: Conference Series*, **985**, 012022(2018), https://doi.org/10.1088/1742-6596/985/1/012022
20. D. Yao, H. Yang, H. Chen, and P. T. Williams, *Applied Catalysis B: Environmental*, **227**, 477(2018), https://doi.org/10.1016/j.apcatb.2018.01.050
21. T. Ahmet and A. Beytullah, *Adsorption Science & Technology*, **19(8)**, 673(2001), https://doi.org/10.1260/0263617011494484
22. D. D. M. Prabaharan, K. Sadaiyandi, M. Mahendran, and S. Sagadevan, *Applied Physics A: Materials Science & Processing*, **123(4)**, (2017), https://doi.org/10.1007/s00339-017-0786-8
23. Z. N. Kayani, M. Z. Butt, S. Riaz, and S. Naseem, *Materials Science-Poland*, **36(4)**, 547(2018), https://doi.org/10.2478/msp-2018-0088
24. I. Graça, M. C. Bacariza, A. Fernandes, and D. Chadwick, *Applied Catalysis B: Environmental*, **224**, 660(2018), https://doi.org/10.1016/j.apcatb.2017.11.009
25. J. Philia, W. Widayat, and S. Sulardjaka, *AIP Conference Proceedings*, **2453**, 020074(2022), https://doi.org/10.1063/5.0094756
26. W. Nabgan, T. A. Tuan Abdullah, R. Mat, B. Nabgan, S. Triwahyono, and A. Ripin, *Applied Catalysis A: General*, **527**, 161(2016), https://doi.org/10.1016/j.apcata.2016.08.033
27. W. Widayat and A. N. Annisa, *AIP Conference Proceedings*, **1904**, 020061(2017), https://doi.org/10.1063/1.5011918
28. E. S. Lokteva and E. V. Golubina, *Pure and Applied Chemistry*, **91(4)**, 609(2019), https://doi.org/10.1515/pac-2018-0715
29. F. Zhang, L. Zhang, Z. Yang, S. Han, Q. Zhu, L. Wang, C. Liu, X. Meng and F. Xiao, *Chinese Journal of Catalysis*, **40(7)**, 1093(2019), https://doi.org/10.1016/S1872-2067(19)63280-8
30. S. Sumari, A. Santoso, R. Cahyanti, Y. Yahmin, and A. R. Wijaya, *AIP Conference Proceedings*, **2251**, 040026(2020), https://doi.org/10.1063/5.0015850
31. R. Dupuis, R. Pellenq, J. B. Champenois, and A. Poulesquen, *The Journal of Physical Chemistry C*, **124(15)**, 8288(2020), https://doi.org/10.1021/acs.jpcc.0c01495
32. H. Dewajani, Rochmadi, S. Purwono, and A. Budiman, *AIP Conference Proceedings*, **1755**, 1(2016), https://doi.org/10.1063/1.4958485
33. A. C. V. Olivares, M. F. Gomez, M. N. Barroso, and M. C. Abello, *International Journal of Industrial Chemistry*, **9(1)**, 61(2018), https://doi.org/10.1007/s40090-018-0135-6
34. S. Munfarida, Widayat, H. Satriadi, B. Cahyono, Hadiyanto, J. Philia, J. Prameswari, *Chemosphere*, **258**, 127274(2020), https://doi.org/10.1016/j.chemosphere.2020.127274
35. T. Nejat, P. Jalalinezhad, F. Hormozi, and Z. Bahrami, *Journal of The Taiwan Institute of Chemical Engineering*, **97**, 216(2019), https://doi.org/10.1016/j.jtice.2019.01.025
36. Y. Lu, H. Jin, and R. Zhang, *Carbon Resources Conversion*, **2(1)**, 95(2019), https://doi.org/10.1016/j.crcon.2019.03.001
37. T. K. R. de Oliveira, M. Rosset, and O. W. Perez-Lopez, *Catalysis Communication*, **104**, 32(2018), https://doi.org/10.1016/j.catcom.2017.10.013
38. W. Widayat, A. Roesyadi, and M. Rachimoellah, *International Journal of Science Engineering*, **4(1)**, 6(2012), https://doi.org/10.12777/ijse.4.1.6-10
39. P. D. Srinivasan, K. Khivantsev, J. M. M. Tengco, H. Zhu, and J. J. Bravo-Suárez, *Journal of Catalysis*, **373**, 276(2019), https://doi.org/10.1016/j.jcat.2019.03.024
40. N. R. Peela, A. Mubayi, and D. Kunzru, *Chemical Engineering Journal*, **167(2–3)**, 578(2011), https://doi.org/10.1016/j.cej.2010.09.081
41. Y. C. Sharma, A. Kumar, R. Prasad, and S. N. Upadhyay, *Renewable and Sustainable Energy Reviews*, **74**, 89(2017), https://doi.org/10.1016/j.rser.2017.02.049

[RJC-6808/2022]